

Article

WC-Co and WC-Co-Cr Coatings for the Protection of API Pipeline Steel from Corrosion in 4% NaCl Solution

El-Sayed M. Sherif ^{1,2,*} , Magdy M. El Rayes ³  and Hany S. Abdo ^{1,4} 

¹ Center of Excellence for Research in Engineering Materials (CEREM), King Saud University, P.O. Box 800, Al-Riyadh 11421, Saudi Arabia; habdo@ksu.edu.sa

² Electrochemistry and Corrosion Laboratory, Department of Physical Chemistry, National Research Centre, El-Behoth St. 33, Dokki, Cairo 12622, Egypt

³ Department of Mechanical Engineering, College of Engineering, King Saud University, P.O. Box 800, Al-Riyadh 11421, Saudi Arabia; melrayes@ksu.edu.sa

⁴ Mechanical Design and Materials Department, Faculty of Energy Engineering, Aswan University, Aswan 81521, Egypt

* Correspondence: esherif@ksu.edu.sa

Received: 22 January 2020; Accepted: 11 March 2020; Published: 16 March 2020



Abstract: Two inorganic coatings, namely 88%WC-12%Co (PSC1) and 86%WC-10%Co-4%Cr (PSC2), were deposited on the surface of an API-2H pipeline steel using high velocity oxy-fuel deposition. The corrosion of the uncoated and coated API-2H steel after their immersion in a solution of 4.0% NaCl for 1 h, 24 h, and 48 h has been studied. Various electrochemical measurements such cyclic potentiodynamic polarization, electrochemical impedance spectroscopy, and potentiostatic current versus time were employed. The surface morphology and analysis were carried out via the use of scanning electron microscopy and energy dispersive X-ray examinations. All experiments have revealed that the deposited coatings decreased the cathodic current, anodic current, corrosion current density (j_{Corr}), absolute current versus time, and the corrosion rate (R_{Corr}) compared to the uncoated API-2H steel. The value of j_{Corr} decreased from 47 $\mu\text{A}/\text{cm}^2$ for uncoated steel to 38 $\mu\text{A}/\text{cm}^2$ for the PSC1-coated steel and 29 $\mu\text{A}/\text{cm}^2$ for the PSC2-coated steel. Moreover, prolonging the time of exposure decreases the j_{Corr} and R_{Corr} values. The j_{Corr} values obtained after 48 h recorded 32, 26, and 20 $\mu\text{A}/\text{cm}^2$ for the uncoated, PSC1, and PSC2 samples, respectively. Moreover, applying these coatings also led to increasing the corrosion resistance (R_p) after all the exposure periods of time. In addition, the PSC2 coating was found to be more protective against corrosion for the surface of the steel than the PSC1 coating.

Keywords: API steel; inorganic coatings; corrosion protection; electrochemical tests; surface analysis

1. Introduction

API pipeline steels are known to be used in numerous applications such as in transportation pipelines, construction and metal processing equipment, off-shore rigs, agitators, pumps, chemical processing equipment, etc. [1–4]. This is because API steels are characterized by excellent toughness, high strength, good weldability, etc. [5–7]. Some of the API steels experience corrosion upon exposure to corrosive environments. Controlling the corrosion control of various grades of API steels in different media were reported in several studies [6–10]. In addition, the influence of the microstructure of API steel on the protective layer generated on its surface after the corrosion in chloride solution was investigated [9]. The effect of changing the microstructure on the behavior of corrosion for the welded joint in the pipeline steel was also reported [11,12], where the corrosion was found to increase.

The failure of steel pipelines mostly takes place as a result of a combination of the uniform corrosion and localized attack [13–16]. This is because the presence of welds within the steel pipelines helps in the occurrence of localized corrosion, which occurs at the area of welds [15,16]. The corrosion behavior of API-2H in sodium chloride solutions using various electrochemical measurements and spectroscopic investigations was reported [17]. The corrosion behavior of the API-2H steel was compared to that of API-4F steel, and it was found that these API steels suffer both uniform and localized corrosion. The severity of the pitting attack was found to decrease with prolonging the immersion time of the steels in the test solution. The study [17] also confirmed that the resistance of API-2H to corrosion was higher than that recorded for API-4F steel.

Herein, two inorganic coatings, namely 86%WC-10%Co-4%Cr and 88%WC-12%Co, were applied on the surface of API-2H pipeline steel. The influence of these coatings on the protection from corrosion of the API-2H steel after exposure to 4.0% NaCl solution for 1.0 h, 24 h, and 48 h was examined. The work herein was carried out using cyclic potentiodynamic polarization (CPP), electrochemical impedance spectroscopy (EIS), and the change of current with time at constant potential (−700 mV (Ag/AgCl)) measurements. The scanning electron (SEM) microscopy and energy-dispersive X-ray (EDX) analyses were used to investigate the surface morphology and elemental analysis, respectively.

2. Experimental Procedures

2.1. Materials and Chemicals

A grade 50 API-2H pipeline steel used herein was purchased from Sunny Steel (Siping Road, Shanghai, China). The chemical composition of the API steel in weight % (wt %) is listed in Table 1. The high velocity oxy-fuel deposition process was employed to apply the 88%WC-12%Co and 86%WC-10%Co-4%Cr coatings onto the surface of the tested steel pipeline. The thicknesses of the 88%WC-12%Co and 86%WC-10%Co-4%Cr applied surface layers were 223 ± 3 and 183 ± 6 μm , respectively. The investigated samples herein are designated as PS, PSC1, and PSC2 for the uncoated API-2H pipeline steel, coated steel with 88%WC-12%Co, and coated steel with 86%WC-10%Co-4%Cr, respectively. The exact chemical composition of the coating layers is recorded in Table 2.

Table 1. Elemental composition for the API-2 H grade 50 steel.

Element	C	Mn	P	S	Si	Cb	Ti	Fe
Wt %	0.14	1.5	0.03	0.015	0.2	0.04	0.02	Balance

Table 2. Main components for the coatings deposited on the surface of the API steel. PSC1: coated steel with 88%WC-12%Co; PSC2: coated steel with 86%WC-10%Co-4%Cr.

Powder Types	WC (wt %)	Co (wt %)	Cr (wt %)
PSC1 coating	88	12	0.0
PSC2 coating	86	10	4.0

2.2. Electrochemical Cell

A three-electrode configuration cell with a capacity of 250 cm³ was utilized for the electrochemical tests. The uncoated and coated API-2H steels were the working electrodes, while the reference and the counter ones were an Ag/AgCl and a Pt sheet, respectively. Both coated and uncoated steels were prepared as working electrodes by welding a wire of copper to the surface of each electrode. Then, the electrodes were mounted using an epoxy resin that was dried spontaneously until being hardened. Only the uncoated steel surface was successively polished with different metallographic grits, up to 1000 emery papers. Before measurements, the working electrodes were degreased with acetone, washed with distilled water, and then left to dry in air.

2.3. Electrochemical Measurements

An Autolab, which was delivered by Metrohm (Utrecht, the Netherlands) was the potentiostat machine employed for the corrosion measurements herein. The plots of the CPP were collected over a potential range from -1200 mV, which was scanned in the anodic direction to reach -0.200 mV (Ag/AgCl). The potential was reversed in the backward direction from a value of -0.200 mV/s to the limit that the reversed direction intersected with the potential of the forward direction. The scan rate for the forward and backward directions was chosen for the steel rods to be 1.67 mV/s [18]. The EIS data were obtained from the corrosion potential (E_{OCP}) of the electrode over a frequency scan from 100 kHz to 1.0 mHz at a ± 5 mV peak-to-peak overlaid AC wave, using the PowerSINE software. The change of current with time curves were collected at a constant value of potential for the steel samples after their immersion in 4% NaCl solution. All electrochemical measurements were performed in triplicate on a fresh surface of the steel electrodes and a new batch of NaCl solutions. The working electrodes were immersed in 4% NaCl solution for 48 h followed by the application of -700 mV for 40 min. Then, their surface morphology was investigated using SEM (JEOL FE-SEM Model 7600, Tokyo, Japan). To obtain the elemental analysis of the corroded surfaces, an EDX (JEOL, Tokyo, Japan) unit attached to the SEM instrument was used.

3. Results and Discussion

3.1. EIS Data

The EIS technique provides necessary kinetic parameters for the corrosion and corrosion protection of metallic materials in corrosive media [19–23]. Typical Nyquist plots measured for (1) PS, (2) PSC1, and (3) PSC2 after the immersion in 4% NaCl solution for 0.1 h are shown in Figure 1. To report the effect of increasing immersion time to 24 h and 48 h, the EIS measurements were obtained for (1) PS, (2) PSC1, and PSC2 after being immersed in 4% NaCl solution for the named time, and the plots are respectively depicted in Figures 2 and 3. All EIS data were analyzed and fitted to the circuit model that is presented in Figure 4, and the impedance values obtained from this fitting process are listed in Table 3. These parameters can be defined as follows: R_S is the resistance of solution, Q represents the constant phase elements, R_p is the polarization resistance, and W is the Warburg impedance [24].

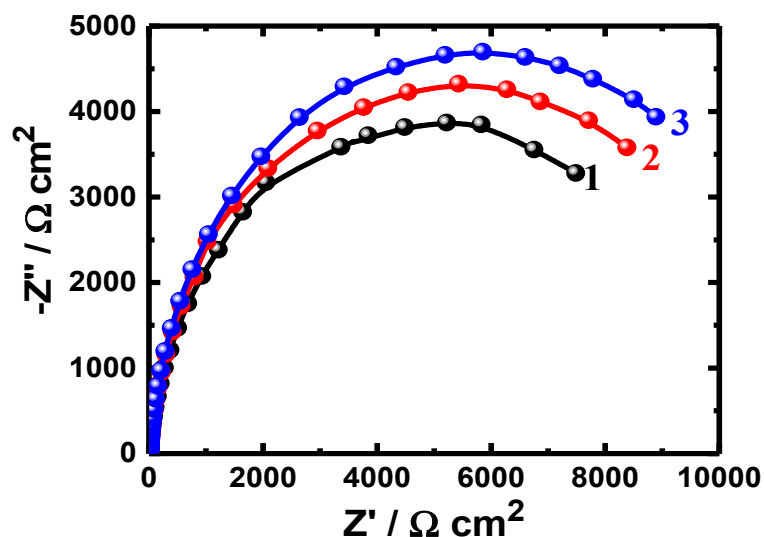


Figure 1. Nyquist plots obtained for (1) PS, (2) PSC1, and (3) PSC2 after their immersion in 4% NaCl solution for 1.0 h.

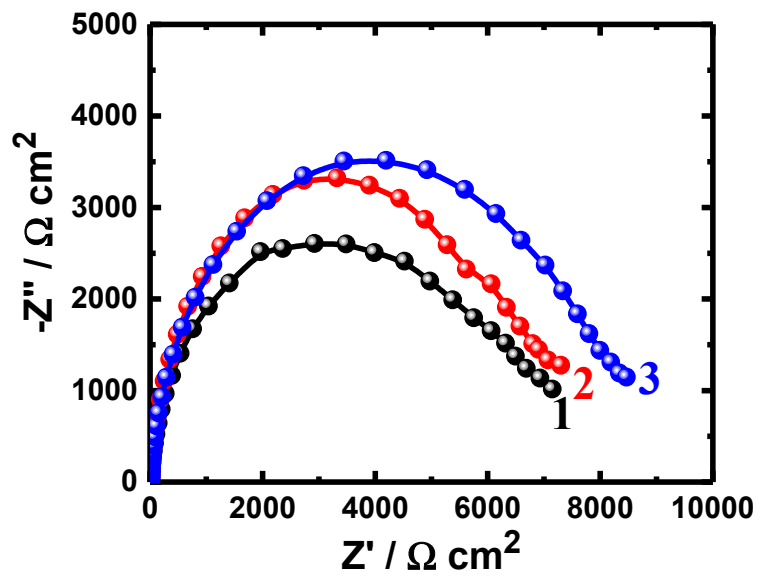


Figure 2. Nyquist plots obtained for (1) PS, (2) PSC1, and (3) PSC2 after their immersion in 4% NaCl solution for 24 h.

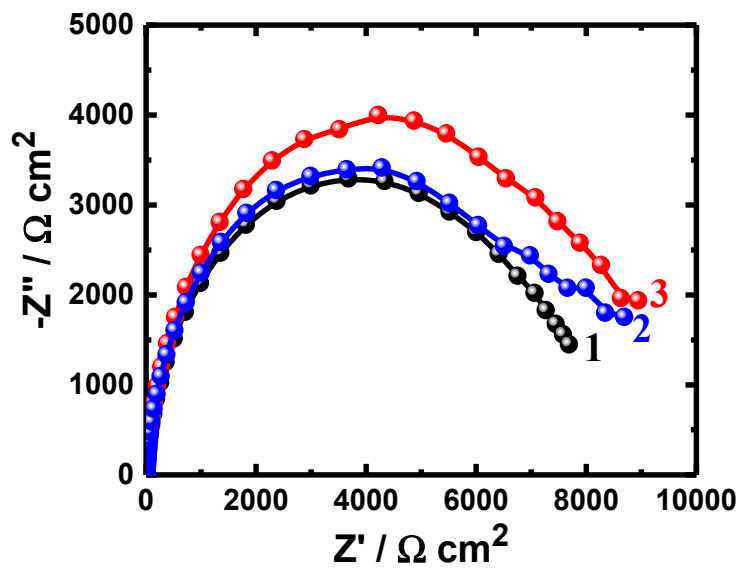


Figure 3. Nyquist plots obtained for (1) PS, (2) PSC1, and (3) PSC2 after their immersion in 4% NaCl solution for 48 h.

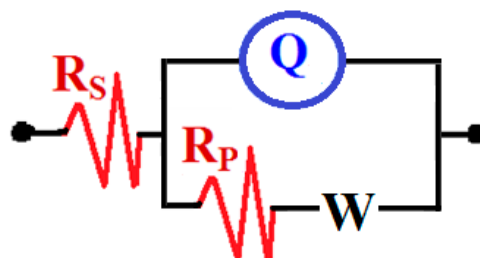


Figure 4. An equivalent circuit model to fit the electrochemical impedance spectroscopy (EIS) experiments shown in Figures 1–3.

Table 3. EIS data obtained for the uncoated and coated steel samples after different immersion periods in 4% NaCl solution.

Sample/Time	$R_s/$ ($\Omega \cdot \text{cm}^2$)	Q		$R_p/$ ($\Omega \cdot \text{cm}^2$)	W/ ($\Omega \cdot \text{cm}^2 \cdot \text{s}^{-\frac{1}{2}}$)
		Y_Q ($Y_Q/S \cdot s^n$)	n		
Uncoated PS (1.0 h)	4.41	0.000214	0.89	3946	0.01867
Coated PSC1 (1.0 h)	3.95	0.000211	0.90	6367	0.01855
Coated PSC2 (1.0 h)	4.41	0.000205	0.90	7091	0.01187
Uncoated PS (24 h)	4.68	0.000188	0.90	4886	0.01098
Coated PSC1 (24 h)	4.76	0.000191	0.91	5647	0.01087
Coated PSC2 (24 h)	5.28	0.000183	0.91	5739	0.01079
Uncoated PS (48 h)	4.75	0.000184	0.91	6634	0.01047
Coated PSC1 (48 h)	4.95	0.000192	0.90	7840	0.00570
Coated PSC2 (48 h)	4.64	0.000181	0.91	7908	0.00635

The obtained Nyquist plots for all samples after immersion for different durations show only one semicircle in the chloride test solutions (Figures 1–3). It is evident from the spectra shown in Figure 1 that the width of the plotted semicircles increases in the order of PS < PSC1 < PSC2. Thus, the corrosion resistance of these materials increases in the same order, i.e., the corrosion resistance increases as PSC2 > PSC1 > PS. Coating the surface of the steel with 88%WC-12%Co increased the corrosion resistance of API-2H steel as a result of the increased passivity of the surface of the steel due to the presence of WC and Co. Furthermore, coating the surface with 86%WC-10%Co-4%Cr provided a higher passivation due to the presence of both WC and Co, in addition to the presence of Cr. Increasing the time of immersion to 24 h and further to 48 h depicted almost the same effect of increasing the resistance of the steel to corrosion, as qualitatively seen in Figures 2 and 3. The increased exposure time was also observed to decrease the diameter of the semicircles for all the uncoated and coated steels, which is most probably because of the increased corrosive attack caused by chloride species toward the steel surfaces.

Figures 1–3 and Table 3 indicate that coating the API steel coated with 88%WC-12%Co showed decreased corrosion, which increased when the steel was coated with 86%WC-10%Co-4%Cr. The parameters listed in Table 3 confirmed also where the polarization resistances (R_p) were greater for the coated electrodes compared to the values obtained for the uncoated ones. The values of the CPE (Q), as represented in Table 3, can be considered as double-layer capacitors having a heavily porous layer. This is because Q , (Y_Q , CPEs), depending on their n -values, can be a W or C_{dl} or a resistor (L); it is W when $n = 0.5$, or C_{dl} with some pores when $n = 1.0$, and L when $n = 0$. Therefore, the values of Y_Q obtained for the coated API-2H steel were much lower than those for the uncoated API-2H steel, which further proves the higher corrosion resistance for the coated API pipeline steel, i.e., PSC1 and PSC2. The presence of W within the equivalent circuit (Figure 4) indicates that the formed layer on the surface of the API steel limits the access of the chloride ions via the mass transport.

Therefore, the EIS data prove that coating the steel with these inorganic coatings protects the steel surface against corrosion by chloride in 4% NaCl solution, owing to API-2H steel forming a top coating layer, which decreases the dissolution of the steel surface via increasing its resistance against the aggressive action of the chloride ions.

3.2. CPP Measurements

To understand the mechanism of the corrosion protection of the API steel through its coating, cyclic polarization measurements were carried out. The CPP curves of (1) PS, (2) PSC1, and (3) PSC2 after immersion for 1.0 h in 4% NaCl solutions are shown in Figure 5. The CPP curves obtained for the same materials after 24 h and 48 h at the same conditions shown respectively in Figures 6 and 7. The values of the Tafel slopes (cathodic (β_c) and anodic (β_a)), corrosion potential (E_{Corr}), the corrosion

current (j_{Corr}) density, and the corrosion resistance (R_p) were calculated as previously reported [19–21] and listed in Table 4.

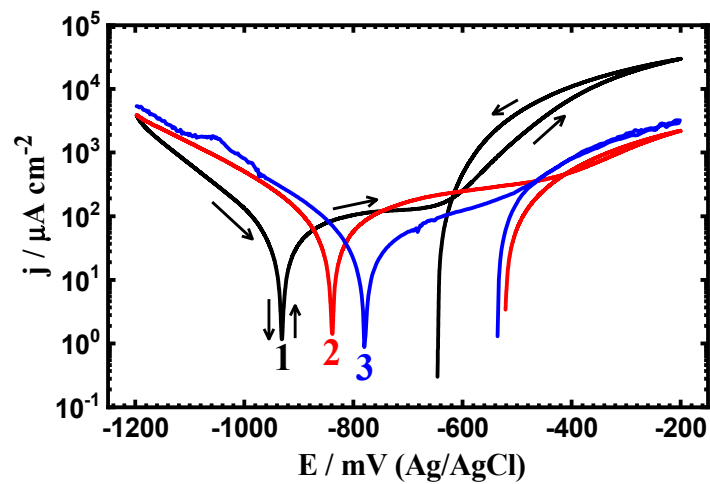


Figure 5. Cyclic potentiodynamic polarization (CPP) measurements obtained for (1) PS, (2) PSC1, and (3) PSC2 in 4% NaCl solution after 1.0 h of exposure.

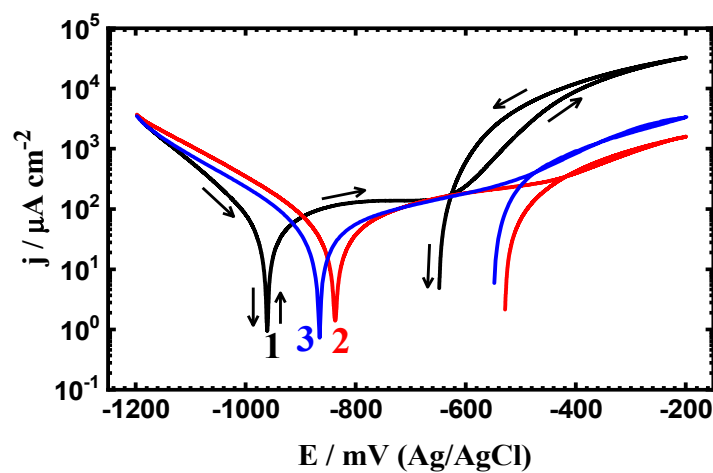


Figure 6. CPP measurements for (1) PS, (2) PSC1, and (3) PSC2 in 4% NaCl solution after 24 h of exposure.

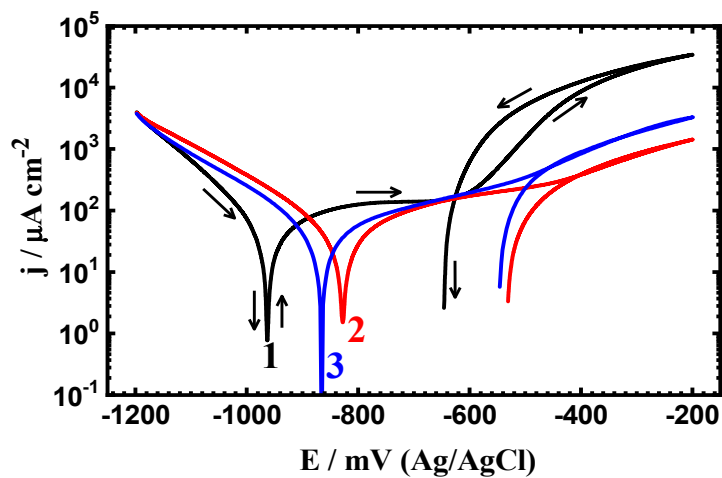


Figure 7. CPP measurements for (1) PS, (2) PSC1, and (3) PSC2 in 4% NaCl solution after 48 h of exposure.

Table 4. Polarization (CPP) data obtained for the PS, PSC1, and PSC2 samples after the different immersion periods in NaCl medium.

Steel/Time	β_c (mV·dec ⁻¹)	E_{Corr} (mV)	β_a (mV·dec ⁻¹)	j_{Corr} ($\mu\text{A}\cdot\text{cm}^{-2}$)	R_p ($\Omega\cdot\text{cm}^2$)	R_{Corr} (mmpy)
Uncoated PS (1.0 h)	105	-928	150	47	531.37	0.545
Coated PSC1 (1.0 h)	100	-840	140	38	667.42	0.441
Coated PSC2 (1.0 h)	95	-780	137	29	841.11	0.336
Uncoated PS (24 h)	125	-958	148	42	718.90	0.371
Coated PSC1 (24 h)	122	-832	142	34	839.14	0.344
Coated PSC2 (24 h)	118	-865	140	28	959.72	0.302
Uncoated PS (48 h)	98	-955	115	32	831.85	0.359
Coated PSC1 (48 h)	110	-825	120	26	994.27	0.325
Coated PSC2 (48 h)	115	-868	125	20	1302.1	0.232

The values of the corrosion rate (R_{Corr}), which are mostly expressing the uniformed corrosion and also listed in Table 4, were calculated using the following equation [25]:

$$R_{Corr} = 3.27 \times 10^{-3} \left(\frac{j_{Corr} E_w}{\rho} \right) \quad (1)$$

where R_{Corr} (millimeters/year), E_w (equivalent weight/grams), ρ (density of the metal or alloy/(g/cm³)), and j_{Corr} ($\mu\text{A}/\text{cm}^2$).

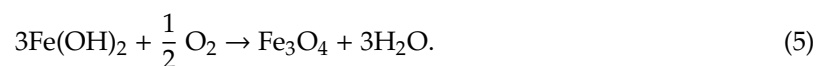
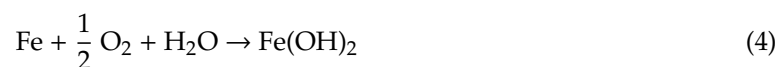
It has been reported that the reaction of cathode for metals and/or alloys in neutral chloride solutions is the reduction of O₂ as per the following equation [26,27];



On another side, the reaction at the anode is the dissolution of metal, which in this case will be the dissolution of Fe presented in the API-2H steel according to the following reaction [27]:



It is evident that the current shows an active passive behavior for all steel samples but the highest current values were recorded for the uncoated steel, PS sample. The active area results due to the iron dissolution to Fe²⁺ and the passivation results from the formation of a corrosion product layer and/or an oxide film onto the steel surface as per the following reactions:



The current continues to increase even in the backward direction, resulting in the creation of an area of a hysteresis loop (curve 1), which is due the pitting attack that takes place on the surface; the massive area of the hysteresis loop indicates that a more severe pitting corrosion takes place. The PSC1 sample shows lower cathodic, anodic, and corrosion currents, a less negative E_{Corr} value, and a smaller hysteresis loop area. The coated PSC2 sample showed the lowest currents, the least negative E_{Corr} value, and the smallest hysteresis loop. This indicates that the severity of both uniform and pitting corrosion decreases with coating, as per the following order; PSC2 < PSC1 < PS.

The exposure period of time was increased to 24 h and 48 h, and the polarization curves are shown respectively in Figures 6 and 7. All CPP plots as well as the corrosion parameters listed in Table 4 indicate that prolonging the time of exposure decreases the corrosion through reducing the values of

j_{Corr} and R_{Corr} , as well as magnifying the R_p values. This confirms that the increase of time decreases the corrosion of all samples, whether uncoated or coated.

3.3. Potentiostatic Current–Time Experiments

The probability of the pitting corrosion to occur for the uncoated and coated steel samples is further explained using the change in the potentiostatic current versus time (PCT) measurements after different exposure periods were utilized. Figure 8 shows the PCT curves obtained for (1) PS, (2) PSC1, and (3) PSC2 after stepping a constant value of potential at -700 mV (Ag/AgCl) in 4% NaCl solution for 1 h. Similar PCT curves were also obtained at the same conditions for the different samples after being exposed to the electrolyte for 24 h and 48 h, as seen respectively in Figures 9 and 10. Figure 8 shows that the initial current values for the uncoated and coated API-2H steels abruptly decreased with time due to a passive film formation. Increasing the time before stepping the potential to the fixed value, -700 mV, led to a slight current decrease until the end of the experiment. It is clear that the uncoated steel sample (PS) recorded the highest absolute currents, while the obtained currents for PSC1 and PSC2 were much lower.

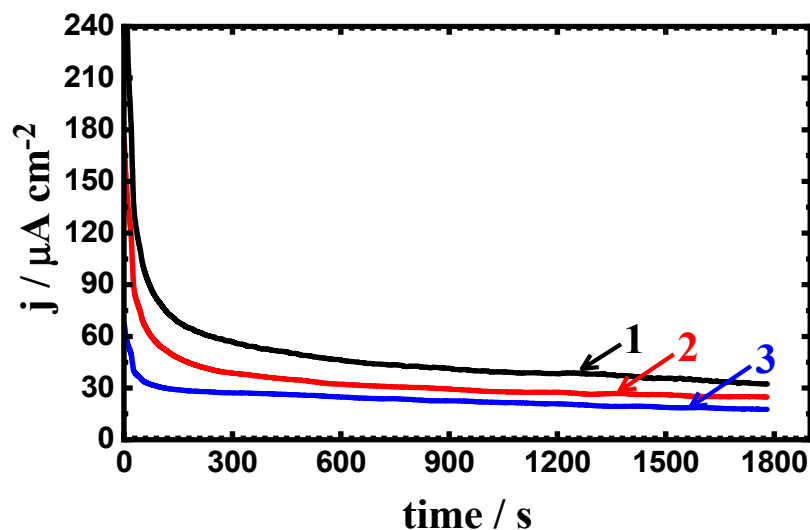


Figure 8. Change of current with time curves for (1) PS, (2) PSC1, and (3) PSC2 at -700 mV in 4% NaCl solution after 1.0 h of exposure.

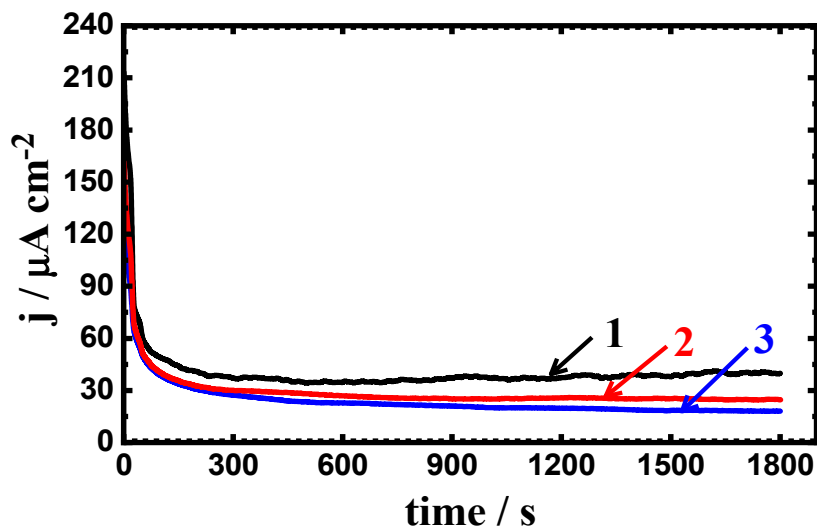


Figure 9. Change of current with time curves for (1) PS, (2) PSC1, and (3) PSC2 at -700 mV in 4% NaCl solution after 24 h of exposure.

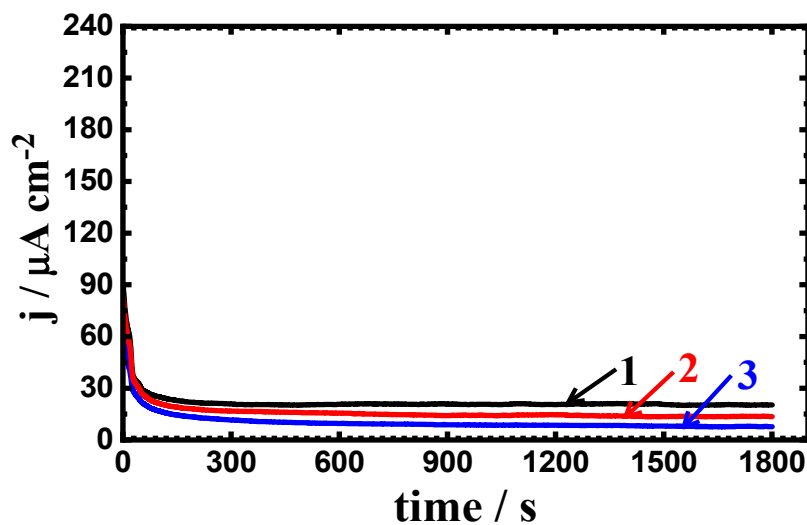


Figure 10. Change of current with time curves for (1) PS, (2) PSC1, and (3) PSC2 at -700 mV in 4% NaCl solution after 48 h of exposure.

Prolonging the exposure time of the steel samples in 4% NaCl solutions to 24 h and 48 h gave almost similar curves but with lower current values (see Figures 9 and 10). Thus, the increase of the exposure time increases the resistance to corrosion for both uncoated and coated steel, where increasing the time has led to increasing the passivity of the steel surfaces. Thus, the current–time behavior for the uncoated and coated steel samples indicates that the pitting corrosion does not occur at this value of the constant potential, i.e., -700 mV (Ag/AgCl).

3.4. SEM and EDX Investigations

The scanning (SEM) and energy-dispersive (EDX) examinations were conducted onto the uncoated and coated steel surfaces to report the corrosion, whether uniform or pitting in 4% NaCl solution at the fixed potential value. Figure 11 depicts (a) the SEM image and (b) its corresponding EDX profile analyses taken from surface of the uncoated API-2H steel (PS) after being in 4% NaCl solution for 48 h, followed by the application of -700 mV for 40 min. It is evident that the surface of the uncoated steel is deteriorated via the corrosive chloride ions attack toward the surface, leading to the formation of corrosion products. Furthermore, the surface does not show any pits, confirming the current–time behavior shown in Figure 10. This occurred although the values of the recorded currents for the uncoated steel electrodes were decreasing with time. The EDX profile analysis presented in Figure 11b shows the spectra for many elements; the weight percentage (*wt %*) for the surface of the uncoated API-2H steel was as follows: 41.91% Fe, 32.84% O, 15.89% C, 6.34% Cl, and 2.56% Na. The high *wt %* of Fe and O indicate that the corrosion product and the top layer formed on the surface of the uncoated API-2H steel were mainly iron oxide (see Equation (5) [28]). The formation of this oxide is not sufficient to fully protect the surface of API-2H steel from corrosion. This is confirmed by the presence of Cl^- in the top layer of the surface of the steel.

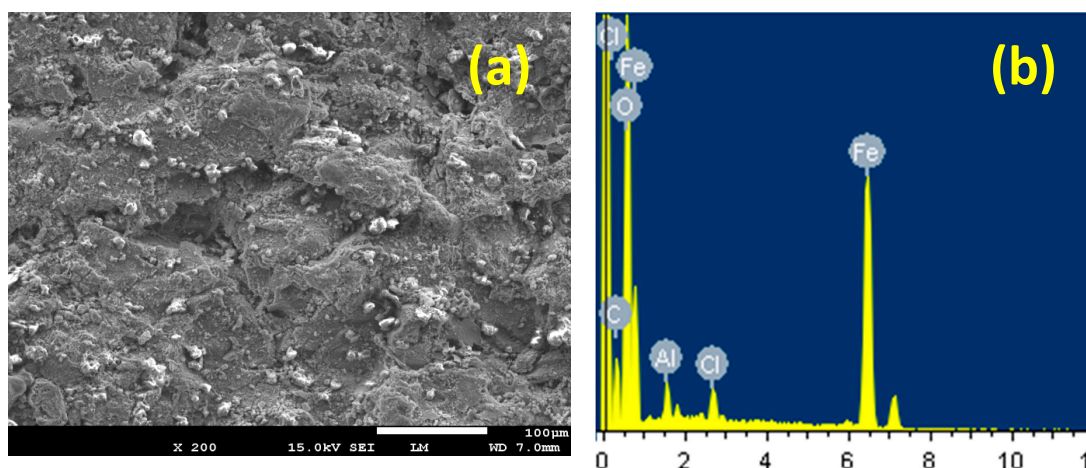


Figure 11. (a) The SEM image and (b) the corresponding energy-dispersive X-ray (EDX) spectra for uncoated PS in 4% NaCl solution for 48 h followed by fixing a potential value of -700 mV for 40 min.

Figure 12a presents the SEM and (b) the EDX spectra for PSC1 in 4% NaCl solution for 48 h followed by fixing a potential value of -0.70 V for 40 min. The SEM image shows a complete coverage for the surface with a thick corrosion product layer. The layer formed here looks denser and more compact compared to the surface of the uncoated steel. The wt % detected for the 88%WC-12%Co coated API-2H steel surface was as follows: 35.97% W, 24.34% C, 13.43% Co, 23.09% O, 1.09% Fe, 0.65% Na, and 0.62% Cl. It is evident that W, C, and Co presented the highest wt % as they are representing the main contents of the coating layer for the PSC1 sample. The presence of a high wt % of O also indicates that the compounds formed on the surface are oxides. Moreover, the presence of a low wt % of iron confirms that the steel surface is well coated with WC-Co coating. Additionally, the existence of both Na and Cl at low wt % reveals the presence of NaCl salt deposited on the surface. The SEM/EDX investigations, along with the current–time measurements obtained for PSC1, thus confirm that coating the API-2H steel with a top layer of WC-Co decreases uniform corrosion and prevents the occurrence of the pitting attack.

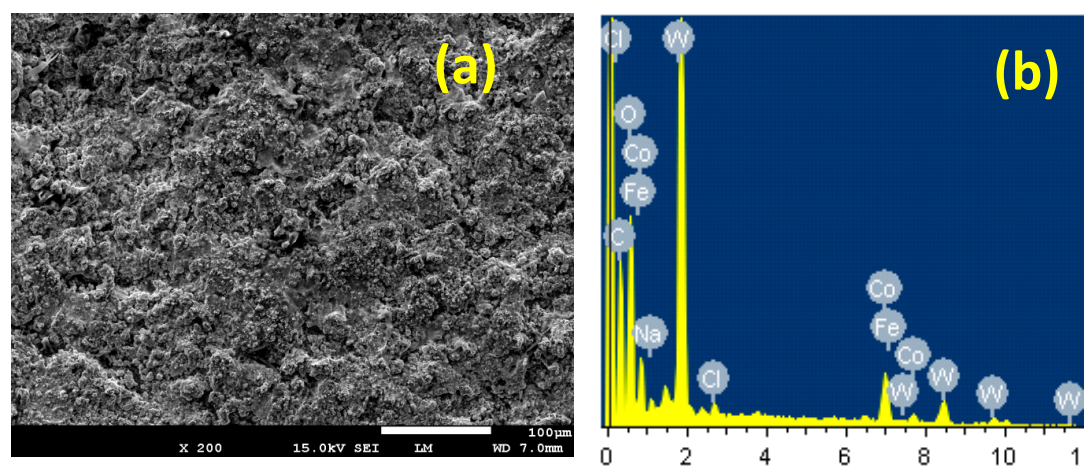


Figure 12. (a) The SEM image and (b) the corresponding EDX spectra for PS coated with 88%WC-12%Co in 4% NaCl solution for 48 h followed by fixing a potential value of -700 mV for 40 min.

Observations of the SEM/EDX investigations are shown in Figure 13; these were performed on the PSC2 sample surface after being exposed to 4% NaCl solution for 48 h and applying -700 mV. It is evident from the SEM micrograph that a thick and dense layer of corrosion products forms on the surface without any indication on the presence of pits inside the formed layer. The wt % obtained from

the EDX profile analysis corresponding to the surface shown in Figure 13 presented these percentages for the element detected: 36.58% W, 29.70% C, 21.60% O, 5.82% Co, 3.02% Cr, 1.96% Na, and 1.31% Cl. The highest wt % was recorded for the main components of the coating layer; i.e., W, C, and O; while a lesser wt % was noted for Co and Cr. This indicates that the addition of 4% Cr to the PSC1 coating to form the PSC2 coating decreases the severity of the steel corrosion in the chloride test solution.

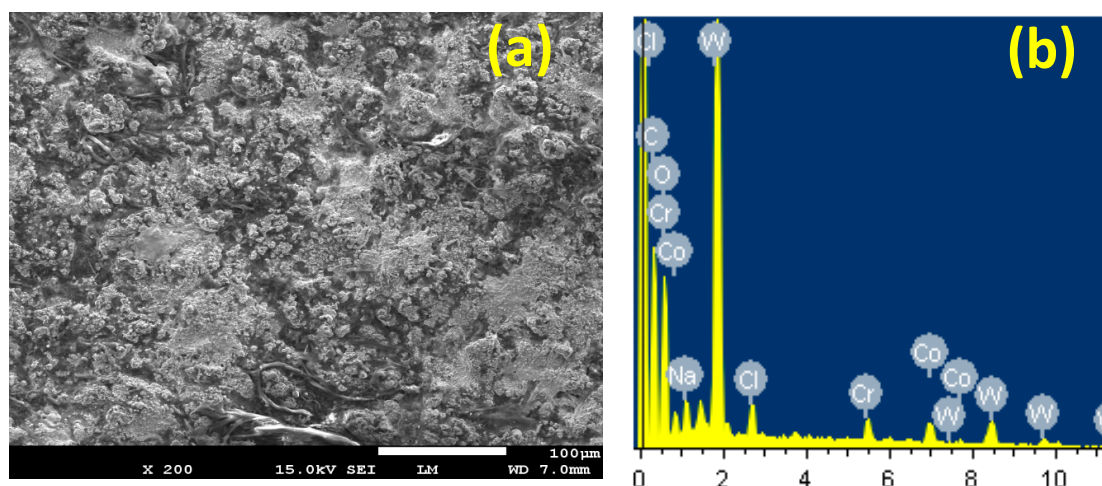


Figure 13. (a) The SEM image and (b) the corresponding EDX spectra for PS coated with 86%WC-10%Co-4%Cr in 4% NaCl solution for 48 h followed by fixing a potential value of -700 mV for 40 min.

4. Conclusions

Two different types of inorganic coatings were synthesized and applied onto the surface of the pipeline API-2H steel (PS). The effect of these coatings on the protection from the corrosion in 4% NaCl solution was investigated by different techniques. It was discovered that the PSC1 and PSC2 coatings decrease the corrosion of the steel through minimizing the anodic and cathodic currents, corrosion current, and the corrosion rate, which in turn increases the resistance to corrosion. The protection from corrosion was due to the surface layer of the coatings that prevents the chloride ions from reaching the steel surface. Protection from corrosion was also confirmed via the SEM micrographs and EDX profile analysis, which indicated the formation of a thick layer that protects the surface of the steel. All the results proved that coating the steel with PSC1 and PSC2 decreased its general corrosion and prevented the pitting attack to take place; however, the PSC2 coating is more protective for the steel surface and thus better than PSC1.

Author Contributions: Conceptualization, E.-S.M.S., H.S.A., and M.M.E.R.; methodology, E.-S.M.S., H.S.A., and M.M.E.R.; validation, E.-S.M.S., H.S.A., and M.M.E.R.; formal analysis, E.-S.M.S., H.S.A., and M.M.E.R.; investigation, E.-S.M.S., H.S.A., and M.M.E.R.; resources, E.-S.M.S. and M.M.E.R.; data curation, E.-S.M.S.; writing—original draft preparation, E.-S.M.S.; writing—review and editing, E.-S.M.S.; supervision, E.-S.M.S. and M.M.E.R.; project administration, E.-S.M.S.; funding acquisition, E.-S.M.S. All authors have read and agreed to the published version of the manuscript.

Funding: This work was funded by the Deanship of Scientific Research at King Saud University via the Research Group Project No. RGP-160.

Acknowledgments: The authors would like to extend their sincere appreciation to the Deanship of Scientific Research at King Saud University for its funding of this research through the Research Group Project No. RGP-160.

Conflicts of Interest: The authors declare no conflict of interest.

References

1. Sherif, E.S.M.; Almajid, A.A. Electrochemical corrosion behavior of API X-70 5L grade steel in 4.0 wt. % sodium chloride solutions after different immersion periods of time. *Int. J. Electrochem. Sci.* **2015**, *10*, 34–45.
2. Sherif, E.S.M.; Almajid, A.A. Anodic dissolution of API X70 pipeline steel in Arabian Gulf seawater after different exposure intervals. *J. Chem.* **2014**, *2014*. [[CrossRef](#)]
3. Guenbour, A.; Hajji, M.A.; Jallouli, E.M.; Bachir, A. Ben Study of corrosion-erosion behaviour of stainless alloys in industrial phosphoric acid medium. *Appl. Surf. Sci.* **2006**, *253*, 2362–2366. [[CrossRef](#)]
4. Hegazy, M.A.; Ahmed, H.M.; El-Tabei, A.S. Investigation of the inhibitive effect of p-substituted 4-(N, N, N-dimethyldodecylammonium bromide)benzylidene-benzene-2-yl-amine on corrosion of carbon steel pipelines in acidic medium. *Corros. Sci.* **2011**, *53*, 671–678. [[CrossRef](#)]
5. Sherif, E.S.; Almajid, A.A.; Khalil, K.A.; Junaedi, H.; Latief, F.H. Electrochemical studies on the corrosion behavior of API X65 pipeline steel in chloride solutions. *Int. J. Electrochem. Sci.* **2013**, *8*, 9360–9370.
6. Zhao, M.C.; Yang, K.; Shan, Y.Y. Comparison on strength and toughness behaviors of microalloyed pipeline steels with acicular ferrite and ultrafine ferrite. *Mater. Lett.* **2003**, *57*, 1496–1500. [[CrossRef](#)]
7. Yakubtsov, I.A.; Poruks, P.; Boyd, J.D. Microstructure and mechanical properties of bainitic low carbon high strength plate steels. *Mater. Sci. Eng. A* **2008**, *480*, 109–116. [[CrossRef](#)]
8. Hernández-Espejel, A.; Domínguez-Crespo, M.A.; Cabrera-Sierra, R.; Rodríguez-Meneses, C.; Arce-Estrada, E.M. Investigations of corrosion films formed on API-X52 pipeline steel in acid sour media. *Corros. Sci.* **2010**, *52*, 2258–2267. [[CrossRef](#)]
9. Alizadeh, M.; Bordbar, S. The influence of microstructure on the protective properties of the corrosion product layer generated on the welded API X70 steel in chloride solution. *Corros. Sci.* **2013**, *70*, 170–179. [[CrossRef](#)]
10. Sherif, E.S.M.; Seikh, A.H. Anodic dissolution in sulfuric acid pickling solutions of the API pipeline X70 grade steel. *Int. J. Electrochem. Sci.* **2015**, *10*, 209–222.
11. Bellaouchou, A.; Kabkab, B.; Guenbour, A.; Ben Bachir, A. Corrosion inhibition under heat transfer of 904L stainless steel in phosphoric acid by benzotriazole. *Prog. Org. Coat.* **2001**, *41*, 121–127. [[CrossRef](#)]
12. Hemmingsen, T.; Hovdan, H.; Sanni, P.; Aagotnes, N.O. The influence of electrolyte reduction potential on weld corrosion. *Electrochim. Acta* **2002**, *47*, 3949–3955. [[CrossRef](#)]
13. Ma, F.Y.; Wang, W.H. Fatigue crack propagation estimation of SUS 630 shaft based on fracture surface analysis under pitting corrosion condition. *Mater. Sci. Eng. A* **2006**, *430*, 1–8. [[CrossRef](#)]
14. Jiang, X.; Zheng, Y.G.; Ke, W. Effect of flow velocity and entrained sand on inhibition performances of two inhibitors for CO₂ corrosion of N80 steel in 3% NaCl solution. *Corros. Sci.* **2005**, *47*, 2636–2658. [[CrossRef](#)]
15. Hardie, D.; Charles, E.A.; Lopez, A.H. Hydrogen embrittlement of high strength pipeline steels. *Corros. Sci.* **2006**, *48*, 4378–4385. [[CrossRef](#)]
16. Kwok, C.T.; Fong, S.L.; Cheng, F.T.; Man, H.C. Pitting and galvanic corrosion behavior of laser-welded stainless steels. *J. Mater. Process. Technol.* **2006**, *176*, 168–178. [[CrossRef](#)]
17. Sherif, E.S.M.; El Rayes, M.M. Corrosion behavior of API 2H and API 4F steels in freely aerated 4.0 % sodium chloride solutions. *Int. J. Electrochem. Sci.* **2015**, *10*, 7493–7504.
18. Poursaee, A. Determining the appropriate scan rate to perform cyclic polarization test on the steel bars in concrete. *Electrochim. Acta* **2010**, *55*, 1200–1206. [[CrossRef](#)]
19. Park, S.M.; Yoo, J.S. Electrochemical impedance spectroscopy for better electrochemical measurements. *Anal. Chem.* **2003**, *75*, 455A–461A. [[CrossRef](#)]
20. Encinas-Sánchez, V.; de Miguel, M.T.; Lasanta, M.I.; García-Martín, G.; Pérez, F.J. Electrochemical impedance spectroscopy (EIS): An efficient technique for monitoring corrosion processes in molten salt environments in CSP applications. *Sol. Energy Mater. Sol. Cells* **2016**, *144*, 109–116. [[CrossRef](#)]
21. Zhao, X.; Qi, Y.; Zhang, Z.; Li, K.; Li, Z. Electrochemical Impedance Spectroscopy Investigation on the Corrosive Behaviour of Waterborne Silicate Micaceous Iron Oxide Coatings in Seawater. *Coatings* **2019**, *9*, 415. [[CrossRef](#)]
22. Barsoukov, E.; Macdonald, J.R. *Impedance Spectroscopy: Theory, Experiment, and Applications*; Wiley & Sons: New York, NY, USA, 1987; ISBN 0471647497.

23. Pan, T.J.; Lu, W.M.; Ren, Y.J.; Wu, W.T.; Zeng, C.L. Electrochemical-impedance-spectroscopy (EIS) study of corrosion of steels 12CrMoV and SS304 beneath a molten ZnCl₂-KCl film at 400 °C in Air. *Oxid. Met.* **2009**, *72*, 179–190. [[CrossRef](#)]
24. Sherif, E.S.M.; Abdo, H.S.; Khalil, K.A.; Nabawy, A.M. Corrosion properties in sodium chloride solutions of Al-TiC composites in situ synthesized by HFIHF. *Metals* **2015**, *5*, 1799–1811. [[CrossRef](#)]
25. Jones, D.A. *Principles and Prevention of Corrosion*, 2nd ed.; Prentice Hall, Inc.: Upper Saddle River, NJ, USA, 1996.
26. Wang, L.; Cheng, L.; Li, J.; Zhu, Z.; Bai, S.; Cui, Z. Combined Effect of Alternating Current Interference and Cathodic Protection on Pitting Corrosion and Stress Corrosion Cracking Behavior of X70 Pipeline Steel in Near-Neutral pH Environment. *Materials* **2018**, *11*, 465. [[CrossRef](#)]
27. Galván-Martínez, R.; Orozco-Cruz, R.; Carmona-Hernández, A.; Mejía-Sánchez, E.; Morales-Cabrera, M.A.; Contreras, A. Corrosion Study of Pipeline Steel under Stress at Different Cathodic Potentials by EIS. *Metals* **2019**, *9*, 1353. [[CrossRef](#)]
28. Sherif, E.-S.M. A Comparative Study on the Electrochemical Corrosion Behavior of Iron and X-65 Steel in 4.0 wt % Sodium Chloride Solution after Different Exposure Intervals. *Molecules* **2014**, *19*, 9962–9974. [[CrossRef](#)]



© 2020 by the authors. Licensee MDPI, Basel, Switzerland. This article is an open access article distributed under the terms and conditions of the Creative Commons Attribution (CC BY) license (<http://creativecommons.org/licenses/by/4.0/>).